


RESEARCH ARTICLE

Open Access



Schisandra chinensis bee pollen's chemical profiles and protective effect against H₂O₂-induced apoptosis in H9c2 cardiomyocytes

Peiyong Shi^{1,2†}, Qianqian Geng^{1,2†}, Lifu Chen^{1,2}, Tianyu Du^{1,2,3}, Yan Lin¹, Rongcai Lai¹, Fei Meng^{1,2,3}, Zhenhong Wu^{1,2}, Xiaoqing Miao^{1,2} and Hong Yao^{4*} 

Abstract

Background: *Schisandra chinensis* (Turcz.) Baill bee pollen extract (SCBPE) is often used as a functional food in China due to its good antioxidant property. However, its chemical compositions and effects on H9c2 cardiomyocytes against H₂O₂-induced cell injury still lacks of reports thus far. This study aimed to characterize the main components of SCBPE and investigate its protective effects against H₂O₂-induced H9c2 cardiomyocyte injury.

Methods: The main components of SCBPE were analyzed via ultraperformance liquid chromatography–quadrupole time-of-flight tandem mass spectrometry (UPLC–QTOF MS/MS). The three main nucleosides in SCBPE were quantitatively analyzed via ultraperformance liquid chromatography–diode array detection. Furthermore, the potential mechanism by which SCBPE exerts protective effects against H₂O₂-induced H9c2 cardiomyocyte injury was explored for the first time via cell survival rate measurements; cell morphological observation; myocardial superoxide dismutase (SOD) activity and malondialdehyde (MDA) and glutathione (GSH) level determination; flow cytometry; and quantitative polymerase chain reaction.

Results: Two carbohydrates, three nucleosides, and nine quinic acid nitrogen-containing derivatives in SCBPE were identified or tentatively characterized via UPLC–QTOF MS/MS. The nine quinic acid nitrogen-containing derivatives were first reported in bee pollen. The contents of uridine, guanosine, and adenosine were 2.4945 ± 0.0185 , 0.1896 ± 0.0049 , and 1.8418 ± 0.0157 µg/mg, respectively. Results of in vitro experiments showed that cell survival rate, myocardial SOD activity, and GSH level significantly increased and myocardial MDA level significantly decreased in SCBPE groups compared with those in H₂O₂ group. Cell morphology in SCBPE groups also markedly improved compared with that in H₂O₂ group. Results indicated that SCBPE protected H9c2 cardiomyocytes from H₂O₂-induced apoptosis by downregulating the mRNA expressions of Bax, cytochrome C, and caspase-3 and upregulating the Bcl-2 mRNA expression.

(Continued on next page)

* Correspondence: hongyao@mail.fjmu.edu.cn

†Peiyong Shi and Qianqian Geng contributed equally to this work.

⁴Department of Pharmaceutical Analysis, School of Pharmacy, Fujian Medical University, 1 Xue Yuan Road, University Town, Fuzhou 350122, People's Republic of China

Full list of author information is available at the end of the article



© The Author(s). 2020 **Open Access** This article is licensed under a Creative Commons Attribution 4.0 International License, which permits use, sharing, adaptation, distribution and reproduction in any medium or format, as long as you give appropriate credit to the original author(s) and the source, provide a link to the Creative Commons licence, and indicate if changes were made. The images or other third party material in this article are included in the article's Creative Commons licence, unless indicated otherwise in a credit line to the material. If material is not included in the article's Creative Commons licence and your intended use is not permitted by statutory regulation or exceeds the permitted use, you will need to obtain permission directly from the copyright holder. To view a copy of this licence, visit <http://creativecommons.org/licenses/by/4.0/>. The Creative Commons Public Domain Dedication waiver (<http://creativecommons.org/publicdomain/zero/1.0/>) applies to the data made available in this article, unless otherwise stated in a credit line to the data.

(Continued from previous page)

Conclusions: This study is the first to report that SCBPE could protect against oxidative stress injury and apoptosis in H₂O₂-injured H9c2 cells. Results indicated that the nucleosides and quinic acid nitrogen-containing derivatives could be the main substances that exert protective effects against H₂O₂-induced H9c2 cardiomyocyte injury.

Keywords: *Schisandra chinensis* bee pollen extract, Nucleosides, Quinic acid nitrogen-containing derivatives, H9c2 cardiomyocytes, H₂O₂, Protective effect

Background

Myocardial ischemia leads to characteristic patterns of metabolic and ultrastructural changes that result in irreversible injury [1]. Patients with acute myocardial ischemic syndromes may represent a continuum of diseases ranging from unstable angina to acute infarction [2], and myocardial infarction is a major cause of death and disability worldwide [3]. Oxidative stress and generation of reactive oxygen species (ROS) can contribute to cardiac ischemic injuries [4, 5]. Excess ROS can induce oxidative modification of cellular macromolecules, inhibit protein functions, and promote cell death [6]. Hydrogen peroxide (H₂O₂), which belongs to O₂-derived nonradical species [6], is a main component of ROS and has been widely used as an inducer of oxidative damage in in vitro models [7]. Various natural products from medicinal plants, such as new depsides from the roots of *Salvia miltiorrhiza* [8], *Dendrobium officinale* polysaccharides [9], chlorogenic acid analogs from *Gynura nepalensis* [10], and bioactive constituents from Chinese propolis [11], have been proved to protect H9c2 cardiomyocytes from H₂O₂-induced oxidative injury.

Bee pollen, which is used as food for all the developmental stages in the hive, is obtained from the agglutination of flower pollens with nectar and salivary substances of the honeybees [12]. Bee pollen extract can be regarded as a promising therapeutic and nutritional natural food supplement because of its certain functions, such as antioxidative, antimicrobial, anti-inflammatory, hepatoprotective, anticancer immunostimulating, and local analgesic effects [13]. These functional biological properties could be due to the high content of flavonoids and polyphenols and considerable radical scavenging capacity [14]. The bee pollen of *Schisandra chinensis* (Turcz.) Baill, which is often used as a functional food in China, has been found to possess a strong antioxidant activity [15–17]. Our recent study revealed the antioxidative and cardioprotective effects of *S. chinensis* bee pollen extract (SCBPE) on isoprenaline-induced myocardial infarction in rats [18]. However, its protective effects against H₂O₂-induced H9c2 cardiomyocyte injury have not been reported yet. This property can also provide scientific evidence for using SCBPE as a functional food for the prevention of myocardial ischemia. With the exception of uridine, which has been isolated from *S.*

chinensis bee pollen [18], the other chemical components of *S. chinensis* bee pollen remain unknown. Identification of these components is beneficial to the further development and utilization of functional foods from *S. chinensis* bee pollen.

High-performance liquid chromatography combined with high-resolution tandem mass spectrometry is a powerful tool for determining the structures of interesting compounds because of its complementary capacity to provide accurate molecular weights and structural information. Numerous medicinal and edible plants have been tested via this technique to disclose their chemical components [19–22]. Ultraperformance liquid chromatography (UPLC) can offer high linear velocities and ultrahigh resolution within a short period of time with little organic solvent consumption. UPLC is especially suitable to the analysis of multiple components in edible and medicinal plants [23, 24]. For example, UPLC methods have been widely adopted for the determination of functional ingredients in chilies [24], apples [25], and oranges [26]. Therefore, UPLC can also be a powerful tool for the quantitative analysis of the interesting ingredients in bee pollen.

In this study, the main components of SCBPE were analyzed via UPLC–quadrupole time-of-flight tandem mass spectrometry (UPLC–QTOF MS/MS). The three main nucleoside components in SCBPE were quantitatively analyzed via UPLC–diode array detection (UPLC–DAD). Furthermore, the potential mechanism by which SCBPE exerts protective effects against H₂O₂-induced H9c2 cardiomyocyte injury was investigated for the first time via cell survival rate measurements; cell morphological observation; myocardial superoxide dismutase (SOD) activity and malondialdehyde (MDA) and glutathione (GSH) level determination; flow cytometry; and quantitative polymerase chain reaction (qPCR).

Methods

Materials and reagents

S. chinensis bee pollen was purchased from an apiary in Xuchang, Henan, China in October, 2015, and stored in 4 °C. The voucher specimens (no. 151001), identified by Prof. Xiaoqing Miao based on China national standard GB/T 30359–2013, are stored in the traditional Chinese medicine pharmacology laboratory of Fujian Agriculture

and Forestry University. Methanol (HPLC-grade) was purchased from Merck (Darmstadt, Germany). Ultra pure water was provided by China Resources C'estbon Beverage (China) Co., Ltd. (Shenzhen, Guangdong, China). Formic acid (HPLC-grade), ethanol and sucrose were obtained from Sinopharm Chemical Reagent Co., Ltd. (Shanghai, China). Uridine, guanosine and adenosine were provided by Solarbio (Beijing, China). The purities of all the standard compounds were determined to be above 98% by HPLC analysis.

Fetal bovine serum (FBS) and Penicillin/Streptomycin (P/S) were purchased from Gibco (USA). Trypsin and Dulbecco's modified Eagle medium (DMEM, high glucose) were purchased from HyClone (USA). 3-(4,5-Dimethylthiazol-2-yl)-2,5-diphenyltetrazolium bromide (MTT) was obtained from Biosharp (China), and 0.4% trypan blue was provided by Solarbio (Beijing, China). The assay kits for MDA, GSH, total SOD, total protein, cell apoptosis (Annexin V-fluorescein isothiocyanate (FITC)/propidium iodide (PI)) were provided by Nanjing Jiancheng Bioengineering Institute (Nanjing, China). Vitamin C (Vc) with the purity of 98% was purchased from Sigma-Aldrich Co. (St. Louis, MO, USA). 30% H₂O₂ solution, dimethylsulfoxide (DMSO), 0.01 M phosphate buffer solution (PBS, pH 7.2–7.4) and other reagents were purchased from Sinopharm Chemical Reagent Co., Ltd. (Shanghai, China).

SCBPE sample preparation

Dry *S. chinensis* bee pollen samples were pulverized into powder, and extracted twice by shaking using a shaker with 70% ethanol at a ratio of 1:15 (w/v) at room temperature for 24 h. After filtration, the extract was centrifuged for 10 min at 7500 g, 4 °C. Then the supernatant was concentrated using a rotary evaporator at 40 °C until the ethanol had been removed. Ultimately, the SCBPE was obtained after lyophilization in a freeze dryer.

For UPLC–QTOF MS/MS and UPLC–DAD analysis, 10 mg of SCBPE sample was accurately weighed and dissolved in 1 mL of 70% aqueous methanol. After vortex for 2 min, the solution was centrifuged at 12704 g for 10 min and 1 µL of supernatant was injected into the UPLC. For the in vitro cell experiment, 100 mg/mL of SCBPE stock solution was prepared using DMSO.

Identification of the main components of SCBPE via UPLC–QTOF MS/MS

UPLC analysis was performed on an Agilent 1290 Infinity LC instrument (Agilent, Waldbronn, Germany) consisting of a quaternary pump, an auto-sampler, a column compartment and a diode-array detector. The samples were separated on a Zorbax SB-C₁₈ column (3.5 µm, 100 mm × 2.1 mm i.d.). The mobile phase was a stepwise gradient of 0.1% formic acid aqueous solution (A) and

methanol (B) as follows: 10% B at 0–3 min; 10–65% B at 3–10 min; 65–80% B at 10–10.5 min and maintained at 80% B from 10.5 min to 15 min. The UV wavelength was set at 254 nm. The column temperature and the flow rate were set at 20 °C and 0.2 mL/min, respectively.

The UPLC system was connected to an Agilent 6530 QTOF mass spectrometer (Santa Clara, CA, USA) equipped with a dual electrospray ionization (ESI) interface using the following operation parameters: capillary voltage, 3.5 kV in (–)ESI mode or 4.0 kV in (+)ESI mode; nebuliser, 40 psig; drying gas (nitrogen) flow rate, 10.0 L/min; gas temperature, 325 °C; fragmentor, 175 V; skimmer voltage, 65 V; OCT 1 RF Vpp, 750 V. Mass spectra were recorded across the range *m/z* 100–1500. The MS/MS collision energy was set at 20–30 V.

Quantitation of three nucleosides from SCBPE via UPLC–DAD

The chromatographic conditions of UPLC–DAD were consistent with those of UPLC–QTOF MS/MS except that the mobile phase has been changed to water (A) and methanol (B).

The stock solution was prepared by dissolving uridine (1.00 mg), guanosine (1.05 mg) and adenosine (1.07 mg) with 70% aqueous methanol in the same one volume flask (2 mL). Then one working solution containing 200 µg/mL of uridine, 210 µg/mL of guanosine and 214 µg/mL of adenosine, which was obtained by diluting the stock solution with 70% aqueous methanol, was further diluted with the same solvent to obtain 9 different concentration levels including 1, 1/2, 1/4, 1/8, 1/16, 1/32, 1/64, 1/128, and 1/256 times of the original concentration to obtain 0.78, 1.56, 3.13, 6.25, 12.5, 25, 50, 100, 200 µg/mL of uridine, 0.82, 1.64, 3.28, 6.56, 13.13, 26.25, 52.5, 105, 210 µg/mL of guanosine, and 0.84, 1.67, 3.34, 6.69, 13.38, 26.75, 53.5, 107, 214 µg/mL of adenosine, respectively. All the solutions were stored at 4 °C before the test. The calibration curve for each ingredient was plotted by using the peak area (*y*) versus concentration (*x*). The limit of detection (LOD) for each component was determined at a signal-to-noise ratio of 3, while the limit of quantification (LOQ) was evaluated at a signal-to-noise ratio of 10. The precision was tested by assaying one concentration of mixed standard solution (100 µg/mL of uridine, 105 µg/mL of guanosine and 107 µg/mL of adenosine) within 1 day in six times, which was measured by relative standard deviation (RSD). To evaluate the repeatability, six SCBPE samples were treated and analyzed with the established method. The RSD was taken as the measure of repeatability. The stability of SCBPE sample solutions was analyzed using the established method at 0, 2, 4, 8, 10, 24, 36, and 48 h, respectively. 10 mg of six SCBPE samples was respectively weighed and spiked with known amounts of reference

compounds, then prepared as described in the Section of SCBPE Sample Preparation and analyzed with the developed UPLC method. The quantity of each compound was subsequently calculated from the corresponding calibration curve. Recovery (%) was calculated by the equation (amount determined - amount original)/amount spiked \times 100%.

Cell culture

Rat-derived H9c2 cardiomyocytes were purchased from Shanghai FuHeng Cell Center (Shanghai, China). Cells were cultured in DMEM (high glucose) supplemented with 10% fetal bovine serum, 1% penicillin and streptomycin at 37 °C in 5% CO₂. Cells were passaged and subcultured to 70–80% confluence with 0.25% trypsin (w/v) every 2–4 days.

Cell viability assay and screening of the appropriate concentration and administration time of SCBPE

H9c2 cells were collected with 0.25% trypsin and resuspended and then seeded in 96-well multiplates with a final density of 5×10^3 cells per well. After incubation for 24 h, cardiomyocytes were pretreated with 6.25, 12.5, 25, 50, 100, 250, 500 μ g/mL of SCBPE for 72 h in order to check the effect of SCBPE on H9c2 cardiomyocytes. Besides, cardiomyocytes were pretreated with 6.25, 12.5, 25, 50, 100, 250, 500 μ g/mL of SCBPE and 40 μ M of Vc for 24 h, 48 h and 72 h, respectively, followed by exposure to 400 μ M of H₂O₂ for 2 h. And cardiomyocytes were pretreated with uridine (0.78–100 μ g/mL), guanosine (0.2–100 μ g/mL), adenosine (0.2–100 μ g/mL) and quinic acid nitrogen-containing derivatives prepared in our laboratory (0.2–25 μ g/mL) for 48 h and 72 h, respectively, followed by exposure to 400 μ M of H₂O₂ for 2 h. Then the MTT assay was performed to detect the cell viability as described previously [9]. Briefly, 10 μ l of 5 mg/mL of MTT solution was added to each well, and the final concentration of MTT was 0.5 mg/mL. After incubation for 4 h under standard condition, 100 μ l of DMSO was added into every well to dissolve the formazan crystals after that the cell supernatants were removed. And the optical density (OD) was measured at 492 nm using a microplate reader Infinite F50 (Tecan, Männedorf, Switzerland). The results of cell viability were expressed as percentages of control.

Morphological changes in myocardial cells

H9c2 cells were collected, re-suspended and seeded in 24-well multiplates for culture, and the morphological changes of the myocardial cells in different groups were observed under the inverted microscope (TS-100F, Nikon).

Determination of SOD activity and MDA and GSH levels

The SOD activity in cultured supernatant and intracellular MDA and GSH levels were determined using commercial kits based on colourimetric methods. After treatment, H9c2 cells in different groups were harvested by centrifugation and the supernatants were used to detect SOD activity. The remaining cells were washed with PBS (pH 7.2–7.4) three times, and then the precipitate obtained through centrifugation was added with PBS (pH 7.2–7.4) and crushed in ice water bath with a manual glass homogenizer. The resulting suspension was collected to analyze the contents of GSH and MDA according to the manufacturer's instructions.

Flow cytometric detection of apoptosis

Apoptosis was detected using an Annexin V-FITC kit according to the manufacturer's recommendations on flow cytometric analysis. After treatment, the H9c2 cells were harvested with non-EDTA trypsin, washed with PBS, and resuspended in binding buffer prior to the addition of Annexin V-FITC and PI. The mixture was incubated for 10 min in the dark at room temperature. Subsequently, cellular fluorescence was measured by flow cytometric analysis using BD Accuri C6 flow cytometer with the C6 Software (BD Biosciences, San Jose, CA, USA).

QPCR

The mRNA expression of caspase-3, cytochrome C, Bax and Bcl-2 in H9c2 myocardial cells was quantified using real time qPCR. Firstly, cells were routinely collected to extract and isolate the total RNA for each treatment group by using the TRIzol reagent (Invitrogen, Carlsbad, CA, USA) in the light of the manufacturer's instruction. Next, the quality of the total RNA isolated (including the content and integrity) were analyzed with spectrophotometry and agarose gel electrophoresis, followed by preparing the cDNA with a commercial kit (*TransScript*[®] One-Step gDNA Removal and cDNA Synthesis Super-Mix; Transgen, China) in line with the production's instructions. QPCR was ultimately carried out on the instrument CFX384 Touch (BIO-RAD laboratories, Inc) with TB Green Premix EX Taq™ II (Tli RNaseH Plus) Kit (Takara, China). GAPDH was used as a housekeeping gene for normalization. The experimental conditions were according to our previous report [27] with a little modification. In brief, the final volume for amplification is 10 μ L including 1 μ L of cDNA template, 0.4 μ L of forward primer, 0.4 μ L of reverse primer, 5 μ L of TB Green premix EX Taq™ II and 3.2 μ L of nuclease-free water. For qPCR, the initial denaturation was fulfilled for 3 min at 95 °C, followed by 40 cycles annealing for 5 s at 95 °C and 30 s at 58 °C with subsequent melting curve analysis, and then increasing the temperature from 65 °C to 95 °C

with a rate of 0.5 °C per 5 s. The mRNA expression levels of caspase-3, cytochrome C, Bax and Bcl-2 in H9c2 were calculated relatively according to that of GAPDH with the $2^{-\Delta\Delta Ct}$ method. All the primers for target genes studied and housekeeping genes were listed as following:

GAPDH (120 bp), forward: 5'-AGCCCAGAACATCA TCCCTG-3',

reverse: 5'-ACGGATACATTGGGGGTAGG-3';

caspase-3 (178 bp), forward: 5'-TCCTGGAGAAATT-CAAGGGA-3',

reverse: 5'-ACGGGATCTGTTTCTTTGCA-3';

cytochrome C (140 bp), forward: 5'-CCTTTGTGGT GTTGACCAGC-3',

reverse: 5'-CCATGGAGGTTTGGTCCAGT-3'.

Bax (154 bp), forward: 5'-ATGTGGATACAGACTC CCCC-3',

reverse: 5'-ATC AGCTCGGGCACTTTAGT-3';

Bcl-2 (264 bp), forward: 5'-AGGGGCTACGAGTGGG ATAC-3',

reverse: 5'-GGACATCTCTGCAAAGTCGC-3';

Statistical analysis

All statistical analyses were performed using Statistical Product and Service Solutions (SPSS) 19.0 software package for Windows (IBM, USA). Values were presented as the mean \pm standard deviation (SD). Statistical significance was performed by one-way analysis of variance (ANOVA). Values with $p < 0.05$ were considered to be statistically significant.

Results

UPLC-ESI-QTOF MS/MS analysis of the main components of SCBPE

The UV chromatogram at 254 nm and total ion current (TIC) chromatograms in positive and negative ion modes of SCBPE are shown in Fig. 1. The data on retention time (t_R), $[M + H]^+$ (or $[M + Na]^+$) ions, $[M - H]^-$ ions, molecular weight, double bond equivalences (DBE), and formula are summarized in Table 1. Q-TOF MS/MS data in negative ESI mode of the components detected in SCBPE are also summarized. Fourteen main components, including two carbohydrates, three nucleosides, and nine quinic acid nitrogen-containing derivatives, were identified or tentatively characterized. Peaks 2, 3, 4, and 5 were confirmed to be sucrose, uridine, adenosine, and guanosine, respectively, by comparing their t_R , MS, and MS/MS data with those of the four reference compounds.

Peak 1 gave an $[M - H]^-$ ion at m/z 195.05159, suggesting that the formula was $C_6H_{12}O_7$ with DBE of 1. It yielded the $[M - H - H_2O]^-$ ion at m/z 177.03972, $[M - H - 2H_2O]^-$ ion at m/z 159.02981, and $[M - H - 2H_2O - CH_2O]^-$ ion at m/z 129.01928 (Additional file 1), which were also found in the MS/MS spectrum of gluconic acid in a previous study [28]. Therefore, according to the formula, DBE, and MS/MS data, peak 1 was tentatively identified as gluconic acid.

Peaks 6, 7, and 9 generated $[M - H]^-$ ions at m/z 704.28380, 704.28298, and 704.28123, respectively, as well as $[M + H]^+$ ions at m/z 706.29816, 706.29697, and

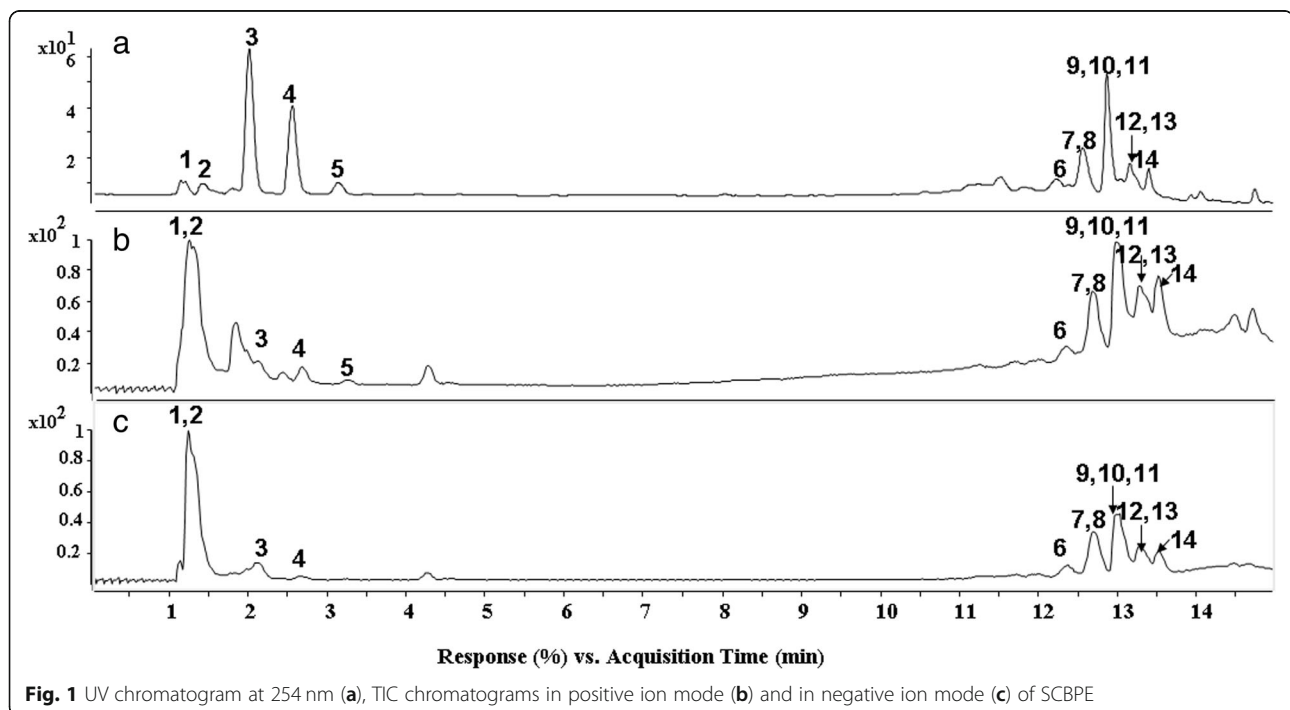


Fig. 1 UV chromatogram at 254 nm (a), TIC chromatograms in positive ion mode (b) and in negative ion mode (c) of SCBPE

Table 1 Peak assignments for the analysis of SCBPE

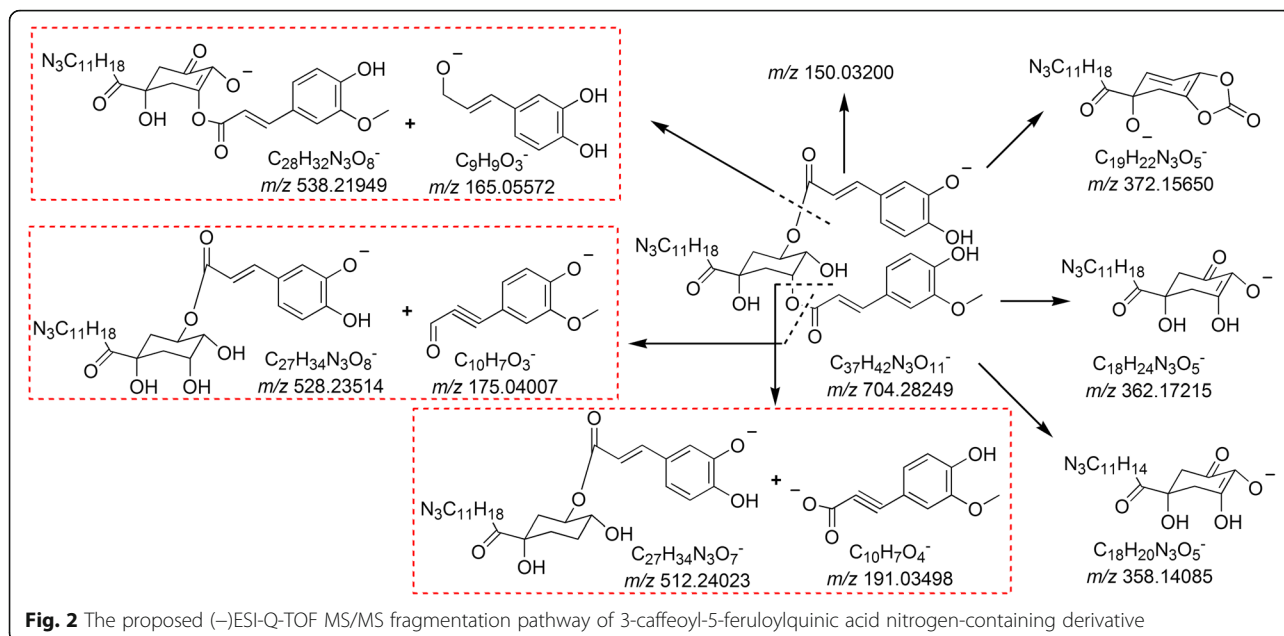
Peak No.	t_R (min)	Identification	(+ ESI-MS m/z)		(- ESI-MS m/z)		DBE	Formula
			Observed	Calculated (Δ ppm)	Observed	Calculated (Δ ppm)		
1	1.239	Gluconic acid			195.05159	195.05103 (-2.89)	1	$C_6H_{12}O_7$
2	1.355	Sucrose ^a	[M + Na] ⁺ 365.10556	365.10543 (0.36)	341.11044	341.10894 (-4.41)	2	$C_{12}H_{22}O_{11}$
3	2.003	Uridine ^a	[M + Na] ⁺ 267.05951	267.05876 (2.81)	243.06264	243.06226 (-1.56)	5	$C_9H_{12}N_2O_6$
4	2.570	Adenosine ^a	268.10476	268.10403 (2.71)	266.08973	266.08948 (-0.94)	7	$C_{10}H_{13}N_5O_4$
5	3.130	Guanosine ^a	284.10797	284.11018 (-7.78)	282.08436	282.08439 (0.11)	7	$C_{10}H_{13}N_5O_5$
6	12.366	Caffeoyl-feruloylquinic acid or caffeoyl-isoferuloylquinic acid nitrogen-containing derivative	706.29816	706.29704 (1.60)	704.28380	704.28249 (1.86)	18	$C_{37}H_{43}N_3O_{11}$
7	12.714	Caffeoyl-feruloylquinic acid or caffeoyl-isoferuloylquinic acid nitrogen-containing derivative	706.29697	706.29704 (-0.09)	704.28298	704.28249 (0.70)	18	$C_{37}H_{43}N_3O_{11}$
8	12.797	Caffeoyl-3'-methoxycinnamylquinic acid or caffeoyl-4'-methoxycinnamylquinic acid nitrogen-containing derivative	690.30371	690.30212 (2.30)	688.28736	688.28757 (-0.31)	18	$C_{37}H_{43}N_3O_{10}$
9	12.979	Caffeoyl-feruloylquinic acid or caffeoyl-isoferuloylquinic acid nitrogen-containing derivative	706.29629	706.29704 (-1.06)	704.28123	704.28249 (-1.79)	18	$C_{37}H_{43}N_3O_{11}$
10	13.079	Caffeoyl-3'-methoxycinnamylquinic acid or caffeoyl-4'-methoxycinnamylquinic acid nitrogen-containing derivative	690.29517	690.30212 (-10.07)	688.28813	688.28757 (0.81)	18	$C_{37}H_{43}N_3O_{10}$
11	13.178	<i>p</i> (or <i>m</i>)-Coumaroyl-3'-methoxycinnamylquinic acid or <i>p</i> (or <i>m</i>)-coumaroyl-4'-methoxycinnamylquinic acid nitrogen-containing derivative	674.30984	674.30721 (3.90)	672.29420	672.29266 (2.29)	18	$C_{37}H_{43}N_3O_9$
12	13.277	Caffeoyl-3'-methoxycinnamylquinic acid or caffeoyl-4'-methoxycinnamylquinic acid nitrogen-containing derivative	690.30160	690.30212 (-0.75)	688.28800	688.28757 (0.63)	18	$C_{37}H_{43}N_3O_{10}$
13	13.244	<i>p</i> (or <i>m</i>)-Coumaroyl-3'-methoxycinnamylquinic acid or <i>p</i> (or <i>m</i>)-coumaroyl-4'-methoxycinnamylquinic acid nitrogen-containing derivative	674.30817	674.30721 (1.42)	672.29314	672.29266 (0.71)	18	$C_{37}H_{43}N_3O_9$
14	13.526	<i>p</i> (or <i>m</i>)-Coumaroyl-3'-methoxycinnamylquinic acid or <i>p</i> (or <i>m</i>)-coumaroyl-4'-methoxycinnamylquinic acid nitrogen-containing derivative	674.30941	674.30721 (3.26)	672.29376	672.29266 (1.64)	18	$C_{37}H_{43}N_3O_9$

^acompared with standard compounds

706.29629, respectively, indicating that they were isomers with the formula of $C_{37}H_{43}N_3O_{11}$. In addition, their MS/MS spectra were identical, suggesting that the three components could possess the same nuclear structure and substituent groups, but the substituted sites of their substituent groups could be different. The (-)ESI-Q-TOF MS/MS spectrum of peak 9 is summarized in Additional file 1 and shown in Additional file 2A. The prominent ions at m/z 538 (base peak) and m/z 165 were a pair of product ions. The formula of the m/z 165 ion was $C_9H_9O_3^-$, indicating that a caffeoyl group might exist in the structure. Moreover, the product ions at m/z 175 and m/z 191 corresponded to $C_{10}H_7O_3^-$ and $C_{10}H_7O_4^-$ ions, respectively, suggesting that another substituent group could be a feruloyl group or an isoferuloyl group; similarly, the ions at m/z 528 and m/z 512 were their corresponding ions, respectively. The m/z 362 product ion with the formula of $C_{18}H_{24}N_3O_5^-$ suggested that a quinic acid nuclear structure was substituted with

a $C_{11}H_{18}N_3$ group. However, numerous substituted sites were found on quinic acid; thus, determining the specific substituted sites according to the MS/MS data was difficult. Hence, peaks 6, 7, and 9 were preliminarily characterized as caffeoyl-feruloylquinic acid or caffeoyl-isoferuloylquinic acid nitrogen-containing derivatives. Nevertheless, these characterization results warrant further investigation. The proposed fragmentation pathway of 3-caffeoyl-5-feruloylquinic acid nitrogen-containing derivative in the negative ion mode is shown in Fig. 2.

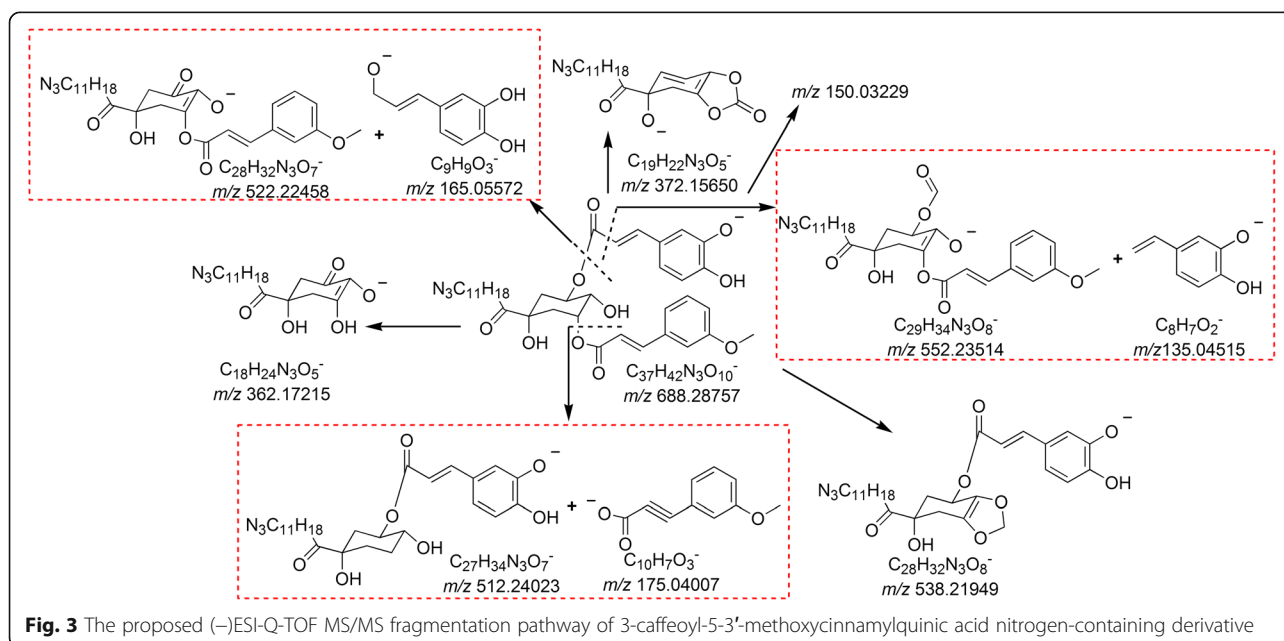
Peaks 8, 10, and 12 gave $[M - H]^-$ ions at m/z 688.28736, 688.28813, and 688.28800, respectively, as well as $[M + H]^+$ ions at m/z 690.30371, 690.29517, and 690.30160, respectively, suggesting that the formula of the three isomers was $C_{37}H_{43}N_3O_{10}$ with a molecular weight 16 Da lower than that of peaks 6, 7, and 9. Moreover, these peaks could be classified as quinic acid nitrogen-containing derivatives. Furthermore, the three components had identical MS/MS spectra. The (-)ESI-



Q-TOF MS/MS spectrum of peak 12 is summarized in Additional file 1 and shown in Additional file 2B. The ions at m/z 165 and m/z 522 were a pair of product ions. The formula of the m/z 165 ion was $C_9H_9O_3^-$, indicating that a caffeoyl group might exist in the structure. The product ion at m/z 175 was attributed to $C_{10}H_7O_3^-$ ion, suggesting that the other substituent group could be a 3'-methoxycinnamyl group or a 4'-methoxycinnamyl group, and the ion at m/z 512 was its corresponding ion. Thus, peaks 8, 10, and 12 could potentially be caffeoyl-3'-methoxycinnamylquinic acid or caffeoyl-4'-

methoxycinnamylquinic acid nitrogen-containing derivatives. The proposed fragmentation pathway of 3-caffeoyl-5-3'-methoxycinnamylquinic acid nitrogen-containing derivative in the negative ion mode is shown in Fig. 3.

Peaks 11, 13, and 14 generated deprotonated molecule $[M - H]^-$ ions at m/z 672.29420, 672.29314, and 672.29376, respectively, as well as $[M + H]^+$ ions at m/z 674.30984, 674.30817, and 674.30941, respectively, indicating that the formula of the three isomers was $C_{37}H_{43}N_3O_9$ with a molecular weight 16 Da lower than



that of peaks 8, 10, and 12. Moreover, they might belong to quinic acid nitrogen-containing derivatives. In addition, the three components had identical MS/MS spectra. The (-)ESI-Q-TOF MS/MS spectrum of peak 14 is summarized in Additional file 1 and shown in Additional file 2C. The m/z 522 ion corresponding to the base peak and the m/z 149 ion were a pair of product ions. The formula of the m/z 149 ion was $C_9H_9O_2^-$, indicating that a *p*-coumaroyl or *m*-coumaroyl group might exist in the structure. The product ion at m/z 175 was the same as that of peaks 8, 10, and 12 in the MS/MS spectra, suggesting that the other substituent group could be a 3'-methoxycinnamyl group or a 4'-methoxycinnamyl group, and the ion at m/z 496 was its corresponding ion. Thus, peaks 11, 13, and 14 were tentatively assigned as *p* (or *m*)-coumaroyl-3'-methoxycinnamylquinic acid or *p* (or *m*)-coumaroyl-4'-methoxycinnamylquinic acid nitrogen-containing derivatives. The proposed fragmentation pathway of 3-3'-methoxycinnamyl-5-*p*-coumaroylquinic acid nitrogen-containing derivative in the negative ion mode is shown in Additional file 3.

To the best of our knowledge, the present study is the first to identify these nine quinic acid nitrogen-containing derivatives from bee pollen.

Quantitative analysis of the three nucleosides of SCBPE via UPLC-DAD

The baseline resolution of uridine, guanosine, and adenosine was obtained (Additional file 4). The calibration curves were $y = 12.114x + 7.4817$ for uridine, $y = 12.916x + 6.6416$ for guanosine, and $y = 10.811x + 4.1441$ for adenosine, and they all displayed good linearity ($R^2 \geq 0.9999$). The LOD of the three nucleosides was 0.195 $\mu\text{g/mL}$. The LOQ of uridine and guanosine was 1.56 $\mu\text{g/mL}$, whereas that of adenosine was 0.78 $\mu\text{g/mL}$. The RSD values of precision were 0.57% for uridine, 0.91% for guanosine, and 0.92% for adenosine, whereas those of repeatability were 1.78% for uridine, 6.93% for guanosine, and 2.14% for adenosine. These values indicated that the method had good precision and repeatability. The RSD values of stability were 1.51% for uridine, 6.85% for guanosine, and 1.96% for adenosine, suggesting that the sample had good stability within 48 h. The average recovery for uridine was 92.87% with RSD of 2.27%, that for guanosine was 99.68% with RSD of 4.99%, and that for adenosine was 102.63% with RSD of 6.31%, demonstrating that the method developed herein was reproducible with good accuracy. The three nucleosides from six SCBPE samples were quantified using this validated method. The contents of uridine, guanosine, and adenosine were 2.4945 ± 0.0185 , 0.1896 ± 0.0049 , and 1.8418 ± 0.0157 $\mu\text{g/mg}$, respectively.

Screening of the appropriate concentration and administration time of SCBPE in vitro

The effects of SCBPE on H9c2 cardiomyocytes for 72 h without H_2O_2 treatment were studied. The OD values

($n = 5$) of the negative control group and 6.25, 12.5, 25, 50, 100, 250, and 500 $\mu\text{g/mL}$ SCBPE groups were 0.6175 ± 0.0034 , 0.5692 ± 0.0031 , 0.5203 ± 0.0079 , 0.5524 ± 0.0078 , 0.5437 ± 0.0056 , 0.5072 ± 0.0102 , 0.5404 ± 0.0012 , and 0.5533 ± 0.0011 , respectively. No significant differences were observed among these groups, suggesting that these SCBPE concentrations could not affect the viability of H9c2 cardiomyocytes. The appropriate concentration and administration time of SCBPE that have an effect on cell vitality were screened via MTT assay. Seven SCBPE concentrations, namely, 6.25, 12.5, 25, 50, 100, 250, and 500 $\mu\text{g/mL}$, and three time periods of 24, 48, and 72 h were tested. As shown in Additional file 5, the OD values of the H_2O_2 group significantly decreased compared with those of the negative control group ($p < 0.01$), suggesting that oxidative injury in H9c2 cells had been induced by 400 μM H_2O_2 for 2 h. Compared with those of the H_2O_2 group, the OD values of the Vc and SCBPE groups pretreated for 48 and 72 h remarkably increased, indicating that Vc and SCBPE could promote cell proliferation. However, the proliferation of myocardial cells pretreated with Vc and SCBPE for 24 h was not evident.

After 48 h pretreatment, both Vc and SCBPE significantly promoted the proliferation of cardiac myocytes ($p < 0.01$). However, the OD values of the Vc and SCBPE groups showed remarkable differences compared with those of the negative control group ($p < 0.01$). By contrast, the proliferation of H_2O_2 -damaged myocardial cells pretreated with Vc and SCBPE (except 500 $\mu\text{g/mL}$) for 72 h was significantly promoted ($p < 0.01$), and the OD values of SCBPE groups (except 250 and 500 $\mu\text{g/mL}$) did not show significant differences compared with those of the negative control group. On the basis of these results, the drug administration for 72 h and concentrations of 12.5, 25, and 50 $\mu\text{g/mL}$ SCBPE were selected for subsequent experiments.

Effects of SCBPE on the survival rate and morphology of H_2O_2 -induced H9c2 cells

As shown in Additional file 6, the survival rate of myocardial cells in the H_2O_2 group was significantly lower than that in the negative control groups ($p < 0.01$). Compared with that of the H_2O_2 group, the cell viability of the Vc group and all the three SCBPE groups significantly increased ($p < 0.01$). Meanwhile, the cell survival rate for 12.5 and 50 $\mu\text{g/mL}$ SCBPE groups was approximate to that for the Vc groups. However, the survival rate for the 25 $\mu\text{g/mL}$ SCBPE group was significantly higher than that for the Vc group ($p < 0.05$).

Microscopic observation revealed that the cell morphology of the negative control group was good, and no abnormal changes were observed. By contrast, microscopic observation showed partial shrinkage of myocardial cells

in the H_2O_2 group. Moreover, the nucleus and cytoplasm vacuoles were dim, the pseudopod disappeared, and intercellular spaces significantly increased. In the Vc and SCBPE groups, Vc and SCBPE had evident reduction effects. The cell morphology and survival rate markedly improved, the shrinking of myocardial cell pseudopodia was not remarkable, and intercellular spaces became smaller and had increased connections (Fig. 4). These results demonstrated the protective effects of SCBPE on H9c2 myocardial cells against H_2O_2 -induced cell injury.

Effects of SCBPE on SOD activity and MDA and GSH levels induced by H_2O_2 in H9c2 cells

After pretreatment for 72 h by different SCBPE concentrations (12.5, 25, and 50 $\mu\text{g}/\text{mL}$) and 40 μM Vc, H9c2 cells were incubated in 400 μM H_2O_2 for 2 h. SOD activity and GSH level were significantly lower ($p < 0.01$) and

MDA level was significantly higher ($p < 0.01$) in the H_2O_2 group than those in the negative control group. SOD activity and GSH level were significantly higher in the 25 and 50 $\mu\text{g}/\text{mL}$ SCBPE groups ($p < 0.05$, $p < 0.01$) than those in the H_2O_2 group. Moreover, MDA level was significantly lower in 40 μM Vc and SCBPE groups ($p < 0.05$, $p < 0.01$) than that in the H_2O_2 group (Table 2).

Effects of SCBPE on apoptosis of H9c2 myocardial cells induced by H_2O_2

The antiapoptotic effects of SCBPE on H9c2 cardiomyocytes against H_2O_2 -induced injury as quantified by the percentage of apoptotic cells were detected by Annexin V-FITC/PI double staining via flow cytometry. As shown in Fig. 5, after 2 h of 400 μM H_2O_2 damage, the apoptosis rate significantly increased in the H_2O_2 group

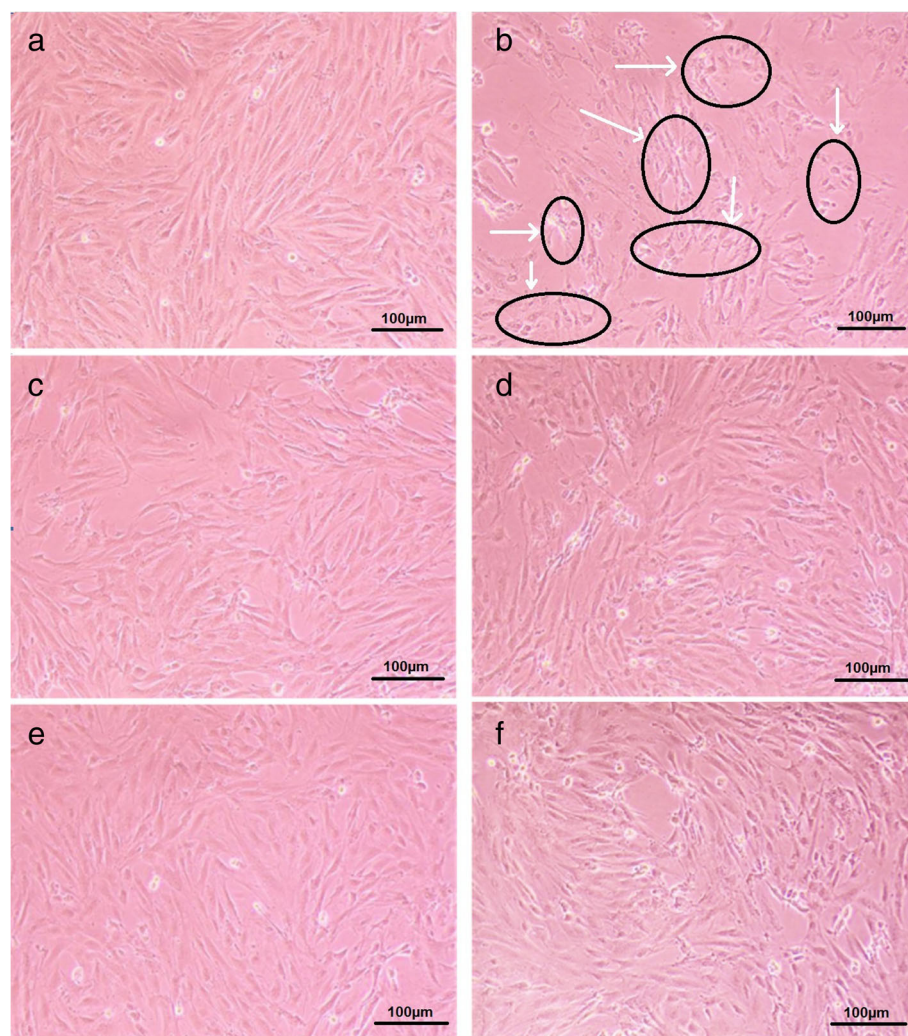


Fig. 4 The effects of SCBPE on morphology of H9c2 myocardial cells. **a**, negative control group; **b**, H_2O_2 group; **c**, positive control (Vc) group; **d**, 12.5 $\mu\text{g}/\text{mL}$ SCBPE; **e**, 25 $\mu\text{g}/\text{mL}$ SCBPE; **f**, 50 $\mu\text{g}/\text{mL}$ SCBPE

Table 2 Effects of SCBPE on SOD activity and MDA and GSH levels induced by H₂O₂ in H9c2 cells

Group	SOD (U/mL) ^a	GSH (μmol/g prot) ^a	MDA (nmol/mg prot) ^a
Negative control group	54.6014 ± 0.2399*	39.8462 ± 1.6048*	0.3034 ± 0.1045*
H ₂ O ₂ group	51.2855 ± 0.4685	26.3654 ± 5.7993	1.4215 ± 0.3413
Positive control (Vc) group	51.9344 ± 0.7776	26.1652 ± 1.3582	0.5677 ± 0.1884*
12.5 μg/mL SCBPE	52.1944 ± 0.5090	36.4072 ± 0.4569#	0.6326 ± 0.1262#
25 μg/mL SCBPE	53.3966 ± 0.4482#	41.3148 ± 2.3994*	0.4958 ± 0.0945*
50 μg/mL SCBPE	52.9136 ± 0.3818#	35.6945 ± 2.7386#	0.5665 ± 0.1061*

^aValues represent mean ± SD of three independent experiments, and *n* = 6 in each experiment. Compared with H₂O₂ group, #*p* < 0.05, **p* < 0.01

(43.93%) compared with that in the negative control group (3.3%) (*p* < 0.01), whereas that of H9c2 cardiomyocytes preincubated with 40 μM Vc and 12.5, 25, and 50 μg/mL SCBPE for 72 h prior to H₂O₂ exposure significantly decreased compared with that in the H₂O₂ group (*p* < 0.01); the percentage of apoptotic cells was 26.33, 28.17, 21.53, and 23.6%, respectively. These results demonstrated that SCBPE inhibited H₂O₂-induced apoptosis in H9c2 cardiomyocytes.

Effects of SCBPE on the mRNA expressions of caspase-3, cytochrome C, Bax, and Bcl-2 of H9c2 myocardial cells induced by H₂O₂

The effects of SCBPE on the mRNA expressions of caspase-3, cytochrome C, Bax, and Bcl-2 on H₂O₂-injured H9c2 cells are illustrated in Fig. 6. The mRNA levels of caspase-3, cytochrome C, and Bax were significantly upregulated and that of Bcl-2 was downregulated in the H₂O₂ group compared with those in the negative control group (*p* < 0.01). Furthermore, the mRNA level ratio of Bcl-2 to Bax markedly decreased. Compared with those in the H₂O₂ group, the mRNA levels of caspase-3, cytochrome C, and Bax were significantly downregulated and that of Bcl-2 was upregulated in the SCBPE groups. Moreover, the mRNA level ratio of Bcl-2 to Bax significantly increased. These results suggested that SCBPE could play a protective role against H₂O₂-induced H9c2 cell injury by regulating the mRNA expressions of caspase-3, cytochrome C, Bax, and Bcl-2, thereby reducing the cell apoptosis caused by H₂O₂.

Discussion

On the basis of the results of cell survival rate measurements and morphological observations, the present study demonstrated the protective effects of SCBPE on H9c2 cardiomyocytes against H₂O₂-induced cell injury. SOD activity and GSH level are also important lines of defense against free radicals [29, 30]. MDA, one of the end products of lipid peroxidation, could lead to severe cell damage by causing polymerization and crosslinking of membrane components, which are recognized as an

indirect oxidative stress marker of cellular injury [11, 31]. Accordingly, SOD activity and GSH and MDA levels are usually used in assessing oxidative stress [27, 30]. In this study, GSH content and SOD activity significantly increased and MDA content decreased in H9c2 cardiomyocytes in the SCBPE groups compared with those in the H₂O₂ group, suggesting that the protective effects of SCBPE against H₂O₂-induced myocardial cell injury could be related to antioxidant activity. These results were consistent with those of our previous research in which we reported that SCBPE could exert antioxidative and cardioprotective effects on isoprenaline-induced myocardial infarction in rats [18].

In addition, two carbohydrates, three nucleosides, and nine quinic acid nitrogen-containing derivatives were identified or tentatively characterized via UPLC–QTOF MS/MS in the present study. The three nucleosides were quantitatively analyzed via UPLC–DAD to reveal the main components of SCBPE. Among the three nucleosides, the contents of adenosine and uridine in SCBPE were 1.8418 ± 0.0157 and 2.4945 ± 0.0185 μg/mg, respectively, which were about 10 and 13 times larger than that of guanosine with 0.1896 ± 0.0049 μg/mg, respectively. Administering an intracoronary infusion of adenosine at a rate of 3.75 mg/min for the first hour of reperfusion after a 90 min left anterior descending occlusion remarkably reduces infarct size and improves regional ventricular function in the ischemic zone in canine preparation [32]. Moreover, intravenous infusion of 0.15 mg/kg/min adenosine results in a sustained reduction in infarct size in a canine model [33]. The Acute Myocardial Infarction Study of Adenosine (AMISTAD) trial by intravenous infusion of adenosine at 70 mg/kg/min for 3 h and AMISTAD-II trial by intravenous infusion of adenosine at 50 mg/kg/min or 70 mg/kg/min for 3 h both demonstrated that adenosine administration with reperfusion therapy can reduce infarct size and improve ventricular function [34–36]. Intravenous infusion of 30 mg/kg uridine can reduce the incidence of ventricular tachycardia and ventricular fibrillation, whereas infusion of uridine during the entire period of acute

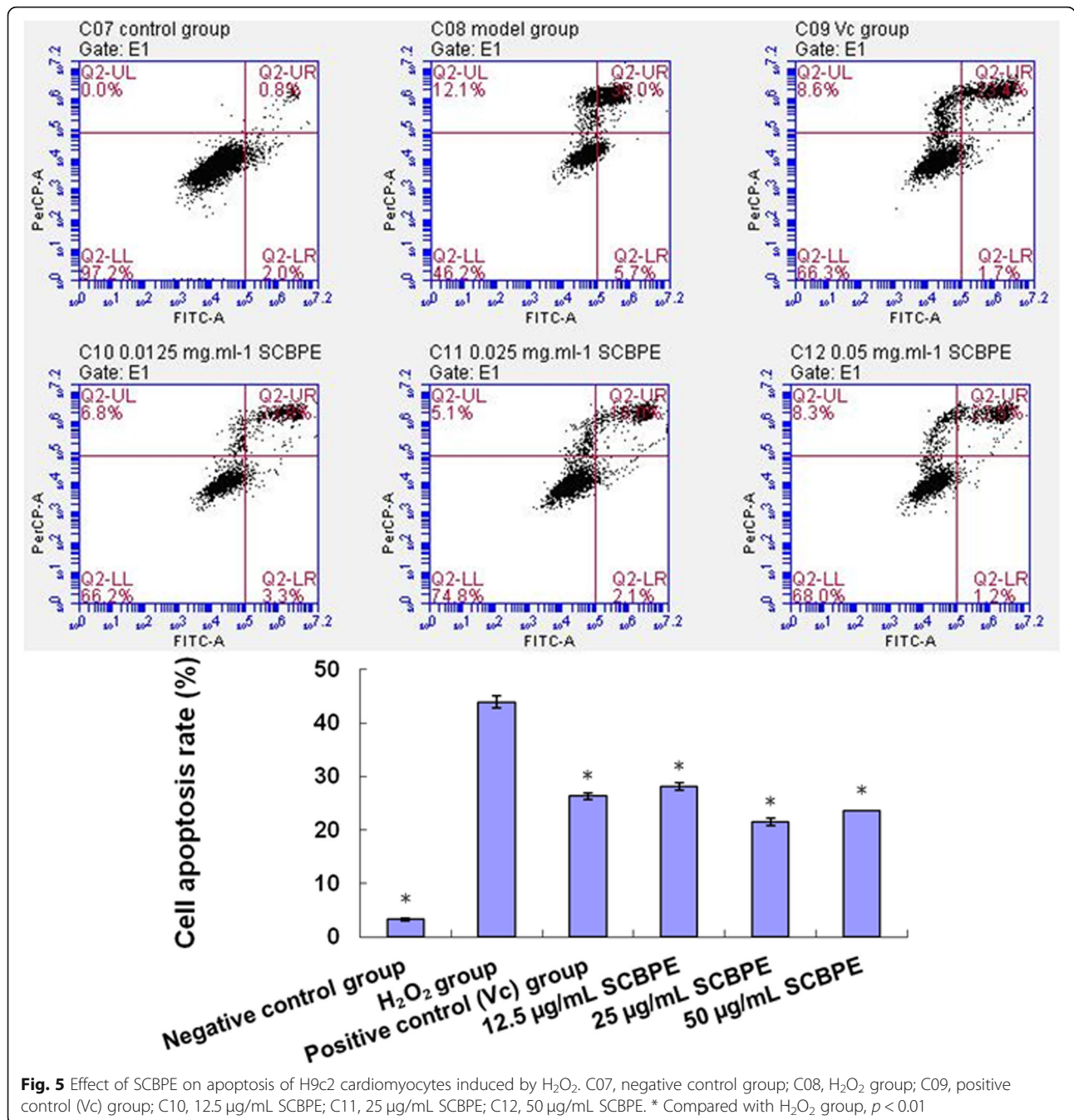


Fig. 5 Effect of SCBPE on apoptosis of H9c2 cardiomyocytes induced by H₂O₂. C07, negative control group; C08, H₂O₂ group; C09, positive control (Vc) group; C10, 12.5 µg/mL SCBPE; C11, 25 µg/mL SCBPE; C12, 50 µg/mL SCBPE. * Compared with H₂O₂ group, *p* < 0.01

myocardial infarction (60 min) would probably contribute to manifestation of antioxidant and anti-ischemic actions [37]. In the present study, nine quinic acid nitrogen-containing derivatives were identified from bee pollen for the first time. Except for the nitrogen-containing group with the molecular composition of C₁₁N₃H₁₈ in the structure, the other substituent groups on quinic acid, namely, caffeoyl, feruloyl (or isoferuloyl), 3'-methoxycinnamyl (or 4'-methoxycinnamyl), and *p*-coumaroyl (or *m*-coumaroyl) groups, have multiple

unsaturated groups in their structure. The presence of these unsaturated groups possibly results in favorable antioxidative capacity. For instance, the caffeoyl–quinic acid group in the structures of peaks 6–10 and 12 reportedly has antioxidative activities [38] and exerts protective effect on cardiomyocytes against oxidative stress-induced damage [10]. Furthermore, the protective effects of uridine, guanosine, adenosine, and quinic acid nitrogen-containing derivatives on H9c2 myocardial cells against H₂O₂-induced cell injury were studied. The cell

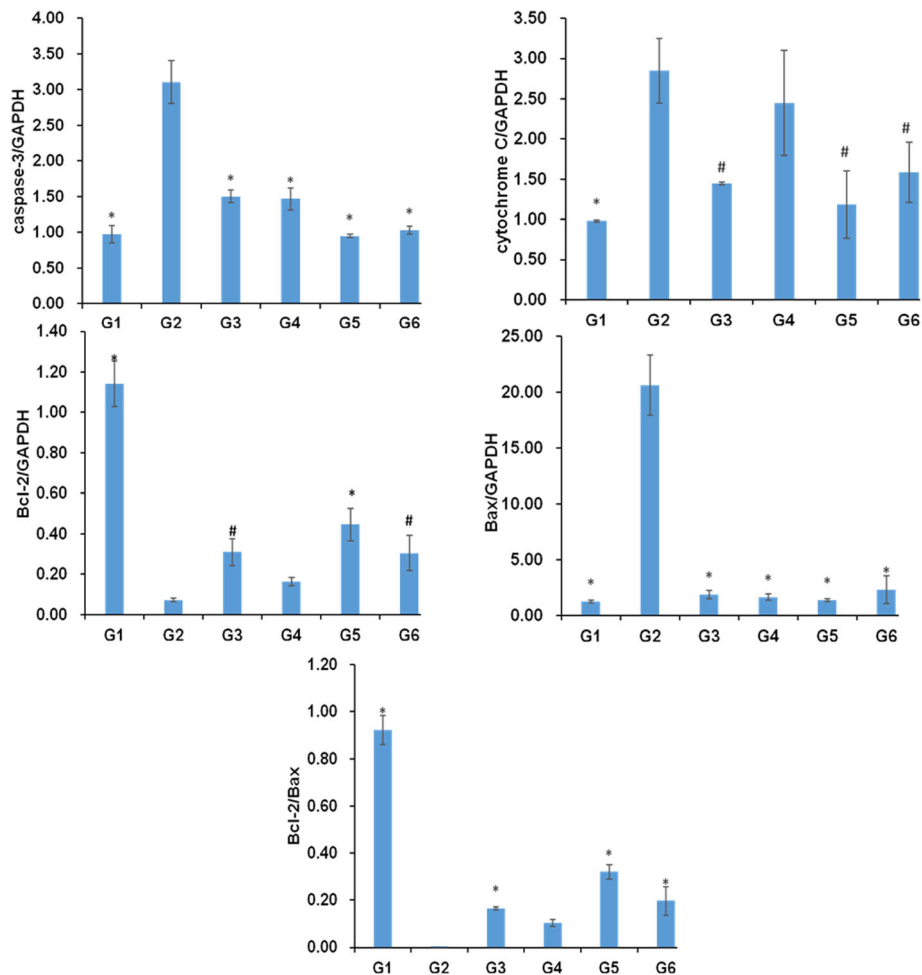


Fig. 6 The effect of SCBPE on the mRNA expression of caspase-3, cytochrome C, Bcl-2, Bax, and Bcl-2/Bax induced by H₂O₂ in H9c2 myocardial cells of each group. G1, negative control group; G2, H₂O₂ group; G3, positive control (Vc) group; G4, 12.5 μg/mL SCBPE; G5, 25 μg/mL SCBPE; G6, 50 μg/mL SCBPE. Compared with H₂O₂ group, # $p < 0.05$, * $p < 0.01$

viability determined via MTT assay is shown in Additional file 7. Compared with those in the H₂O₂ group, the OD values significantly increased in the adenosine groups (0.2–100 μg/mL for 48 h and 0.78–25 [except for 6.25 μg/mL] for 72 h), uridine groups (100 μg/mL for 48 h and 25–100 μg/mL for 72 h), guanosine groups (0.2–3.125 μg/mL for 48 h and 0.39 and 1.56 μg/mL for 72 h), and nitrogen-containing quinic acid derivative groups (0.2–12.5 μg/mL for 48 h and 0.2–6.25 μg/mL for 72 h). Therefore, the main nucleosides and quinic acid nitrogen-containing derivatives could be the main active components of SCBPE against H₂O₂-induced H9c2 cardiac cell injury.

Oxidative stress mediated by ROS can trigger myocyte apoptosis, which could be one of the major mechanisms in myocardial ischemia injury [9, 39]. Once ROS are generated, they can increase mitochondrial permeability, resulting in cytochrome C release.

Bcl-2 family member proteins can regulate the release of mitochondrial cytochrome C during oxidative stress in cardiomyocytes, and cell survival may increase when Bcl-2 expression is relatively high but only when Bax expression is low [40]. Hence, the ratio of Bax to Bcl-2 is an effective predictor of the apoptotic fate of cardiomyocytes [41, 42]. Subsequently, cytochrome C can form a complex with caspase-9 and APAF-1, leading to caspase-9 activation. In turn, caspase-9 can activate the executioner caspases (caspase-3, -6, and -7) and induce cell death [10, 43]. Several studies reported that H₂O₂ exposure can induce cardiomyocyte apoptosis [39] and substantially increase the levels of Bax and caspase-3 and decrease the level of Bcl-2 in H9c2 cells [40]. The present study demonstrated that SCBPE remarkably inhibited cardiomyocyte apoptosis induced by H₂O₂ by downregulating Bax, cytochrome C, and caspase-3 mRNA expression and upregulating Bcl-2 mRNA expression.

Conclusion

In this study, two carbohydrates, three nucleosides, and nine quinic acid nitrogen-containing derivatives were identified or tentatively characterized in SCBPE via UPLC–QTOF MS/MS. The nine quinic acid nitrogen-containing derivatives were reported in bee pollen for the first time. Three nucleosides, namely, uridine, guanosine, and adenosine, were quantitatively analyzed via UPLC–DAD. Results showed that SCBPE could reduce oxidative stress-induced apoptosis in H9c2 cells by downregulating Bax, cytochrome C, and caspase-3 mRNA expression and upregulating Bcl-2 mRNA expression. These findings indicated that SCBPE exerts protective effects on H9c2 cells against oxidative stress and apoptosis in vitro, and the main nucleosides and quinic acid nitrogen-containing derivatives could be the primary pharmacodynamic substances involved in this mechanism.

Supplementary information

Supplementary information accompanies this paper at <https://doi.org/10.1186/s12906-020-03069-1>.

Additional file 1: (–)ESI-Q-TOF MS/MS data of peaks 1, 9, 12 and 14 of SCBPE.

Additional file 2: (–)ESI-Q-TOF MS/MS spectra of peaks 9 (A), 12 (B) and 14 (C).

Additional file 3: The proposed (–)ESI-Q-TOF MS/MS fragmentation pathway of 3–3'-methoxycinnamyl-5-p-coumaroylquinic acid nitrogen-containing derivative.

Additional file 4: UPLC–DAD Chromatograms at 254 nm of the mixed reference substances including 25 µg/mL of uridine, 26.25 µg/mL of guanosine and 26.75 µg/mL of adenosine (A) and SCBPE (B).

Additional file 5: Effect of seven concentrations of SCBPE on proliferation of H9c2 cells induced by H₂O₂ in three time periods, respectively.

Additional file 6: The effect of SCBPE on cell survival rate of H9c2 cells. * Compared with H₂O₂ group, $p < 0.01$. # SCBPE+H₂O₂ groups compared with Vc + H₂O₂ group, $p < 0.05$.

Additional file 7: Effect of adenosine, guanosine, uridine and nitrogen-containing quinic acid derivatives on H₂O₂-induced H9c2 myocardial cell injury, respectively.

Abbreviations

DBE: Double bond equivalences; ESI: Electrospray ionization; FITC: Fluorescein isothiocyanate; GSH: Glutathione; H₂O₂: Hydrogen peroxide; MDA: Malondialdehyde; MTT: 3-(4,5-dimethylthiazol-2-yl)-2,5-diphenyltetrazolium bromide; OD: Optical density; PI: Propidium iodide; ROS: Reactive oxygen species; RSD: Relative standard deviation; SCBPE: *Schisandra chinensis* bee pollen extract; SOD: Superoxide dismutase; TIC: Total ion current; Vc: Vitamin C

Acknowledgements

Not applicable.

Authors' contributions

PS, HY and XM conceived and designed the experiments. PS, QG, LC, TD and FM performed the experiments. PS, QG, YL and RL analyzed the data. PS and QG wrote the manuscript. ZW and HY revised the manuscript. All authors read and approved the final version of the manuscript.

Funding

The authors gratefully acknowledge the Natural Science Foundation of Fujian Province (2018 J01596), the Modern Agro-industry Technology Research System (CARS-45-KXJ20), the National Nature Science Foundation of China (81973558), the Training Program for Excellent Scientific Research Talents of Young Teachers in Fujian Province University (2017), the Program for New Century Excellent Talents in Fujian Province University (2018), and the Joint Funds for the Innovation of Science and Technology, Fujian province (2017Y9123). The funders had no role in study design, data collection and analysis, decision to publish, or preparation of the manuscript.

Availability of data and materials

The datasets used or analyzed during the study are available from the corresponding author on reasonable request.

Ethics approval and consent to participate

Not applicable.

Consent for publication

Not applicable.

Competing interests

The authors declare that they have no competing interests.

Author details

¹Department of Traditional Chinese Medicine Resource and Bee Products, College of Animal Sciences (College of Bee Science), Fujian Agriculture and Forestry University, Fuzhou, China. ²State and Local Joint Engineering Laboratory of Natural Biotoxins, Fujian Agriculture and Forestry University, Fuzhou, China. ³College of Food Science, Fujian Agriculture and Forestry University, Fuzhou, China. ⁴Department of Pharmaceutical Analysis, School of Pharmacy, Fujian Medical University, 1 Xue Yuan Road, University Town, Fuzhou 350122, People's Republic of China.

Received: 20 November 2019 Accepted: 1 September 2020

Published online: 10 September 2020

References

- Buja LM. Myocardial ischemia and reperfusion injury. *Cardiovasc Pathol*. 2005;14(4):170–5.
- Ohman EM, Armstrong PW, Christenson RH, Granger CB, Katus HA, Hamm CW, et al. Cardiac troponin T levels for risk stratification in acute myocardial ischemia. *N Engl J Med*. 1996;335(18):1333–41.
- Thygesen K, Alpert JS, Jaffe AS, Simoons ML, Chaitman BR, White HD, et al. Third universal definition of myocardial infarction. *Circulation*. 2012;126(16):2020–35.
- Levrant J, Iwase H, Shao ZH, Vanden Hoek TL, Schumacker PT. Cell death during ischemia: relationship to mitochondrial depolarization and ROS generation. *Am J Physiol Heart Circ Physiol*. 2003;284(2):H549–58.
- Misra MK, Sarwat M, Bhakuni P, Tuteja R, Tuteja N. Oxidative stress and ischemic myocardial syndromes. *Med Sci Monit*. 2009;15(10):RA209–19.
- Circu ML, Aw TY. Reactive oxygen species, cellular redox systems, and apoptosis. *Free Radic Biol Med*. 2010;48(6):749–62.
- Sim MO, Jang JH, Lee HE, Jung HK, Cho HW. Antioxidant effects of *Geranium nepalense* ethanol extract on H₂O₂-induced cytotoxicity in H9c2, SH-SY5Y, BEAS-2B, and HEK293. *Food Sci Biotechnol*. 2017;26(4):1045–53.
- Zhang JQ, Jin QH, Deng YP, Hou JJ, Wu WY, Guo DA. New depsides from the roots of *Salvia miltiorrhiza* and their radical scavenging capacity and protective effects against H₂O₂-induced H9c2 cells. *Fitoterapia*. 2017;121:46–52.
- Zhao XY, Dou MM, Zhang ZH, Zhang DD, Huang CZ. Protective effect of *Dendrobium officinale* polysaccharides on H₂O₂-induced injury in H9c2 cardiomyocytes. *Biomed Pharmacother*. 2017;94:72–8.
- Yu BW, Li JL, Guo BB, Fan HM, Zhao WM, Wang HY. Chlorogenic acid analogues from *Gynura nepalensis* protect H9c2 cardiomyoblasts against H₂O₂-induced apoptosis. *Acta Pharmacol Sin*. 2016;37(11):1413–22.
- Sun LP, Wang K, Xu X, Ge MM, Chen YF, Hu FL. Potential protective effects of bioactive constituents from Chinese propolis against acute oxidative stress induced by hydrogen peroxide in cardiac H9c2 cells. *Evid Based Complement Alternat Med*. 2017;2017:7074147.

12. Pascoal A, Rodrigues S, Teixeira A, Feas X, Estevinho LM. Biological activities of commercial bee pollens: antimicrobial, antimutagenic, antioxidant and anti-inflammatory. *Food Chem Toxicol.* 2014;63:233–9.
13. Komosinska-Vashev K, Olczyk P, Kazmierczak J, Mencner L, Olczyk K. Bee pollen: chemical composition and therapeutic application. *Evid Based Complement Alternat Med.* 2015;2015:297425.
14. Denisow B, Denisow-Pietrzyk M. Biological and therapeutic properties of bee pollen: a review. *J Sci Food Agric.* 2016;96(13):4303–9.
15. He W, Xu X, Sun LP, Pang J, Mu XF, Huang L, et al. Antioxidant activity of four kinds of bee pollen oil. *Food Sci.* 2011;32(17):114–7.
16. Zhang H, Dong J, Ren X, Qin J. Antioxidant activities of ethanol extracts from ten kinds of bee pollens. *Food Sci.* 2008;29(10):75–9.
17. Zhang HC, Wang X, Wang K, Li CY. Antioxidant and tyrosinase inhibitory properties of aqueous ethanol extracts from monofloral bee pollen. *J Agric Sci.* 2015;59(1):119–28.
18. Shen ZH, Geng QQ, Huang HB, Yao H, Du TY, Chen LF, et al. Antioxidative and cardioprotective effects of *Schisandra chinensis* bee pollen extract on isoprenaline-induced myocardial infarction in rats. *Molecules.* 2019;24(6):1090.
19. Hwang YH, Ma JY. Preventive effects of an UPLC-DAD-MS/MS fingerprinted hydroalcoholic extract of *Citrus aurantium* in a mouse model of ulcerative colitis. *Planta Med.* 2018;84(15):1101–9.
20. Shoko T, Maharaj VJ, Naidoo D, Tselanyane M, Nthambeleni R, Khorombi E, et al. Anti-aging potential of extracts from *Sclerocarya birrea* (a. rich.) Hochst and its chemical profiling by UPLC-Q-TOF-MS. *BMC Complement Altern Med.* 2018;18:54.
21. Nemattallah KA, Ayoub NA, Abdelsattar E, Meselhy MR, Elmazar MM, El-Khatib AH, et al. Polyphenols LC-MS² profile of Ajwa date fruit (*Phoenix dactylifera* L.) and their microemulsion: potential impact on hepatic fibrosis. *J Funct Foods.* 2018;49:401–11.
22. Yao H, Chen B, Zhang YY, Ou HG, Li YX, Li SG, et al. Analysis of the total biflavonoids extract from *Selaginella doederleinii* by HPLC-QTOF-MS and its in vitro and in vivo anticancer effects. *Molecules.* 2017;22(2):325.
23. D'Archivio AA, Di Donato F, Foschi M, Maggi MA, Ruggieri F. UHPLC analysis of saffron (*Crocus sativus* L.): optimization of separation using chemometrics and detection of minor crocetin esters. *Molecules.* 2018;23(8):1851.
24. Schmidt A, Fiechter G, Fritz EM, Mayer HK. Quantitation of capsaicinoids in different chilies from Austria by a novel UHPLC method. *J Food Compos Anal.* 2017;60:32–7.
25. Tian Y, Gou XJ, Niu PF, Sun LJ, Guo YR. Multivariate data analysis of the physicochemical and phenolic properties of not from concentrate apple juices to explore the alternative cultivars in juice production. *Food Anal Methods.* 2018;11(6):1735–47.
26. Zhao ZY, He SS, Hu Y, Yang Y, Jiao BN, Fang Q, et al. Fruit flavonoid variation between and within four cultivated *Citrus* species evaluated by UPLC-PDA system. *Sci Hortic.* 2017;224:93–101.
27. Huang HB, Shen ZH, Geng QQ, Wu ZH, Shi PY, Miao XQ. Protective effect of *Schisandra chinensis* bee pollen extract on liver and kidney injury induced by cisplatin in rats. *Biomed Pharmacother.* 2017;95:1765–76.
28. Felipe DF, Brambilla LZS, Porto C, Pilau EJ, Cortez DAG. Phytochemical analysis of *Pfaffia glomerata* inflorescences by LC-ESI-MS/MS. *Molecules.* 2014;19(10):15720–34.
29. da Costa MFB, Liborio AB, Teles F, Martins CD, Soares PMG, Meneses GC, et al. Red propolis ameliorates ischemic-reperfusion acute kidney injury. *Phytomedicine.* 2015;22(9):787–95.
30. Huang HB, Geng QQ, Yao H, Shen ZH, Wu ZH, Miao XQ, et al. Protective effect of scutellarin on myocardial infarction induced by isoprenaline in rats. *Iran J Basic Med Sci.* 2018;21(3):267–76.
31. Chang RM, Li Y, Yang XX, Yue Y, Dou LL, Wang YW, et al. Protective role of deoxyschizandrin and schisantherin A against myocardial ischemia-reperfusion injury in rats. *PLoS One.* 2013;8(4):e61590.
32. Olafsson B, Forman MB, Puett DW, Pou A, Cates CU, Friesinger GC, et al. Reduction of reperfusion injury in the canine preparation by intracoronary adenosine: importance of the endothelium and the no-reflow phenomenon. *Circulation.* 1987;76(5):1135–45.
33. Pitarys CJ 2nd, Virmani R, Vildibill HD Jr, Jackson EK, Forman MB. Reduction of myocardial reperfusion injury by intravenous adenosine administered during the early reperfusion period. *Circulation.* 1991;83(1):237–47.
34. Mahaffey KW, Puma JA, Barbagelata NA, DiCarli MF, Leeser MA, Browne KF, et al. Adenosine as an adjunct to thrombolytic therapy for acute myocardial infarction: Results of a multicenter, randomized, placebo-controlled trial: The Acute Myocardial Infarction Study of Adenosine (AMISTAD) trial. *J Am Coll Cardiol.* 1999;34(6):1711–20.
35. Ross AM, Gibbons RJ, Stone GW, Kloner RA, Alexander RW, AMISTAD-II Investigators. A randomized, double-blinded, placebo-controlled multicenter trial of adenosine as an adjunct to reperfusion in the treatment of acute myocardial infarction (AMISTAD-II). *J Am Coll Cardiol.* 2005;45(11):1775–80.
36. Forman MB, Stone GW, Jackson EK. Role of adenosine as adjunctive therapy in acute myocardial infarction. *Cardiovasc Drug Rev.* 2006;24(2):116–47.
37. Bul'on W, Krylova IB, Selina EN, Rodionova OM, Evdokimova NR, Sapronov NS, et al. Antiarrhythmic effect of uridine and uridine-5'-monophosphate in acute myocardial ischemia. *Bull Exp Biol Med.* 2014;157(6):728–31.
38. Hung TM, Na MK, Thuong PT, Su ND, Sok DE, Song KS, et al. Antioxidant activity of caffeoyl quinic acid derivatives from the roots of *Dipsacus asper* wall. *J Ethnopharmacol.* 2006;108(2):188–92.
39. Han SY, Li HX, Ma X, Zhang K, Ma ZZ, Tu PF. Protective effects of purified safflower extract on myocardial ischemia *in vivo* and *in vitro*. *Phytomedicine.* 2009;16(8):694–702.
40. Zhang Q, Huang WD, Lv XY, Yang YM. Ghrelin protects H9c2 cells from hydrogen peroxide-induced apoptosis through NF-κB and mitochondria-mediated signaling. *Eur J Pharmacol.* 2011;654(2):142–9.
41. Condorelli G, Morisco C, Stassi G, Notte A, Farina F, Sgarbetta G, et al. Increased cardiomyocyte apoptosis and changes in proapoptotic and antiapoptotic genes bax and bcl-2 during left ventricular adaptations to chronic pressure overload in the rat. *Circulation.* 1999;99(23):3071–8.
42. Zhao Y, Xu Y, Zhang J, Ji T. Cardioprotective effect of carvedilol: inhibition of apoptosis in H9c2 cardiomyocytes via the TLR4/NF-κB pathway following ischemia/reperfusion injury. *Exp Ther Med.* 2014;8(4):1092–6.
43. Zaman S, Wang R, Gandhi V. Targeting the apoptosis pathway in hematologic malignancies. *Leuk Lymphoma.* 2014;55(9):1980–92.

Publisher's Note

Springer Nature remains neutral with regard to jurisdictional claims in published maps and institutional affiliations.

Ready to submit your research? Choose BMC and benefit from:

- fast, convenient online submission
- thorough peer review by experienced researchers in your field
- rapid publication on acceptance
- support for research data, including large and complex data types
- gold Open Access which fosters wider collaboration and increased citations
- maximum visibility for your research: over 100M website views per year

At BMC, research is always in progress.

Learn more biomedcentral.com/submissions

